Thermochimica Acta, 86 (1985) 77–84
Elsevier Science Publishers B.V., Amsterdam – Printed in The Netherlands

STUDY OF THE THERMAL DECOMPOSITION OF IRON AND BARIUM CITRATES *

A. SRIVASTAVA, P. SINGH, V.G. GUNJIKAR and A.P.B. SINHA
National Chemical Laboratory, Pune 411 008 (India)
(Received 25 September 1984)

ABSTRACT

Iron citrate decomposes to give α-Fe_2O_3 as an end product at 460°C via a four-step process. Barium citrate has been found to decompose to a stable barium carbonate at 412°C. It is, however, observed that a mixture of iron and barium citrates decomposes to BaO and either γ-Fe_2O_3 or Fe_3O_4 or a mixture of these two oxides. Thus, the mixture does not decompose to give α-Fe_2O_3 and $BaCO_3$ as obtained in the individual decomposition of iron citrate and barium citrate, respectively. The iron and barium oxides obtained as a result of decomposition of the mixture then chemically combine to form barium ferrite at 600°C.

INTRODUCTION

The most common method for preparing oxide electroceramics such as ferrites which serve as raw materials in the fabrication of permanent magnets involves the calcination of a mechanically ground mixture of metal oxides and carbonates at very high temperatures.

In the present work, a non-conventional method is used for the preparation of barium ferrite, a commonly used permanent magnet material. This method is known as the "Liquid mix technique" [1,2] and it involves the formation of citrates of iron and barium individually, mixing them in solution, calcining to burn off all the organic material and chemically combining the oxides. This method showed great potential for obtaining high uniformity and homogeneity of the product formed as the ions are mixed on an atomic level in the liquid state. This method does not involve milling of the compound as is required in the ceramic method to produce fine-grained powders. This is an advantage of this method as milling introduces lattice defects and strains in the compound which have a detrimental effect on the permanent magnet properties. The barium ferrite formed by this method is ideally suited to studies of its basic properties. In

* NCL Communication No. 3591.

0040-6031/85/$03.30

view of this, it appeared necessary to study the preparation and decomposition of the amorphous citrate salts, i.e., iron citrate, barium citrate and a stoichiometric combination of iron citrate and barium citrate, to enable a systematic study of the various properties of barium ferrite.

EXPERIMENTAL

Preparation

The chemicals used in the preparation were iron citrate (Riedel–Dettaen, Seelze–Hannover, AG) barium carbonate (BDH, AR) and citric acid (HPC, LR).

In order to prepare a stoichiometric mixture of iron and barium citrates, the required amounts of iron citrate and barium carbonate were accurately weighed. A solution of iron citrate was prepared in distilled water. An aqueous solution of barium citrate was also prepared in the following way: a concentrated solution of citric acid was made in distilled water. Small amounts of the barium carbonate were added to this citric acid solution with constant stirring, resulting in a colourless solution of a barium citrate complex. The two solutions, i.e., of iron citrate and barium citrate, thus formed were then mixed together, again with continuous stirring. The mixture was heated over a hot-plate at a temperature of about 40°C. At the end of the heating, the product remaining was in the form of a solid mass which was glass-like in nature. This homogeneous glassy mixture was then subjected to differential thermal analysis (DTA). To support the thermogravimetric data, infrared (IR) spectroscopy and X-ray diffraction (XRD) were used in the study.

Instrumental

A Netzch STA 409 differential thermal analyser was used to obtain the thermal data on the citrates. This differential thermal analyser simultaneously plots the results of differential thermal analysis (DTA), thermogravimetric analysis (TGA) and derivative thermogravimetric analysis (DTG) along with the sample temperature (T). The IR spectra were recorded in nujol on a Pye Unicam IR spectrometer (SP3-300). For recording the X-ray diffraction patterns, a Philips 1730 diffractometer was used.

For the differential thermal analysis, 50 mg of the sample were placed in an cylindrical-type platinum crucible mounted on one of the 2-mm alumina rods of the sample carrier covering the Pt/Pt–10% Rh differential thermocouple which measured the sample temperature simultaneously. The sample was heated in a dynamic air atmosphere at a rate of 10°C min^{-1} and a chart speed of 120 mm h^{-1} was used during the thermogravimetric scan.

The activation energies for the various decomposition steps were calculated from the DTA data using the following formula [3]

$$\frac{\log \mathrm{d}w/\mathrm{d}t}{\log W_r} \text{ vs. } \frac{(T^{-1})}{\log W_r}$$

where W = total weight loss up to time t, $W_r = W_c - W$, W_c = weight loss at completion of reaction, T = absolute temperature.

RESULTS AND DISCUSSION

The DTA studies on iron citrate ($FeC_6H_5O_7 \cdot 2H_2O$) showed that the decomposition of iron citrate to iron oxide (α-Fe_2O_3) as the end product is a four-step process as shown in the thermogravimetric curve (TG) in Fig. 1.

In the first step (step A) an endothermic change having an activation energy of 31.8 kcal mol^{-1} leading to dehydration was observed in the temperature range 22–175°C. This dehydration begins at 35°C and is completed by 175°C. The IR spectrum (Fig. 2) of the sample obtained at the end of this stage is similar to that of the starting material except for the sharpening of the bands and a reduction in the hydroxyl band intensity. As seen from the spectrum, there are two hydroxyl bands appearing at 3460 and

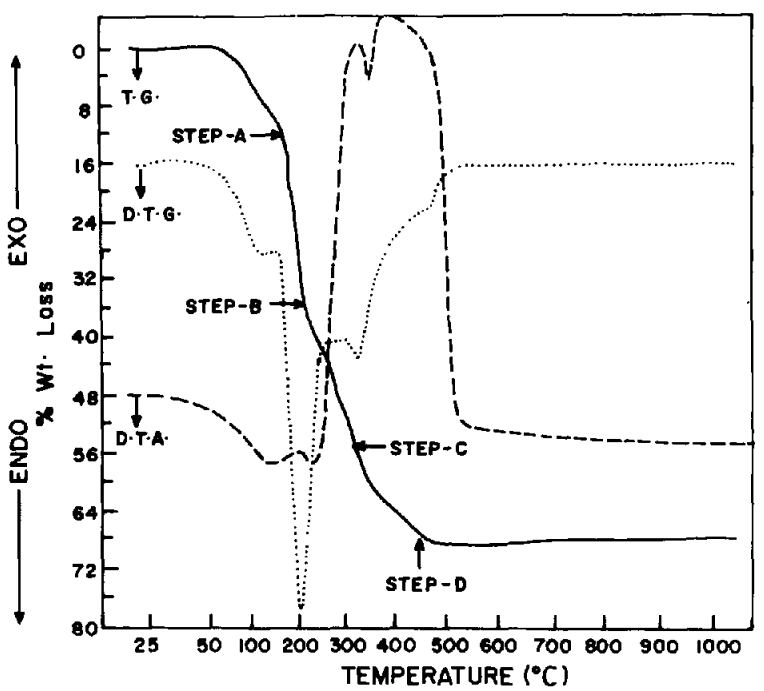

Fig. 1. TG, DTG, DTA curves of iron citrate in air.

3220 cm^{-1} corresponding to the weakly bonded water of crystallization and the hydroxyl group in the molecule. Therefore the observed weight loss (13.0%) in this step may be attributed only to the removal of two molecules of crystal water leading to a calculated loss of 12.9%.

The IR spectrum (Fig. 2) of the sample after the second step (step B) of the TG curve in the temperature range 175–228°C still showed the presence of the hydroxyl stretching band and the carboxylate band at 3220 and 1580 cm^{-1}, respectively, in addition to all other bands corresponding to those present in the IR spectrum of the first step, but with reduced intensities. The observed weight loss of 20.2% for this step is due, therefore, to partial decarboxylation of the citrate moiety which agrees with the weight loss of 20.0% calculated for the loss of one carboxyl group per citrate moiety. As seen in the DTA curve the reaction in this decomposition step is exothermic having an activation energy of 10.6 kcal mol^{-1}.

The third step of the decomposition curve (step C) in the temperature range 228–330°C is also exothermic with an activation energy of 33.4 kcal mol^{-1} giving rise to a weight loss of 20.4%. The IR spectrum (Fig. 2) corresponding to this step showed the absence of the –OH band and a considerable reduction in the intensities of all the bands. Therefore, the loss in weight in this step can be attributed to further decarboxylation of the citrate moiety. The observed and calculated weight loss tally has been summarised in Table 1.

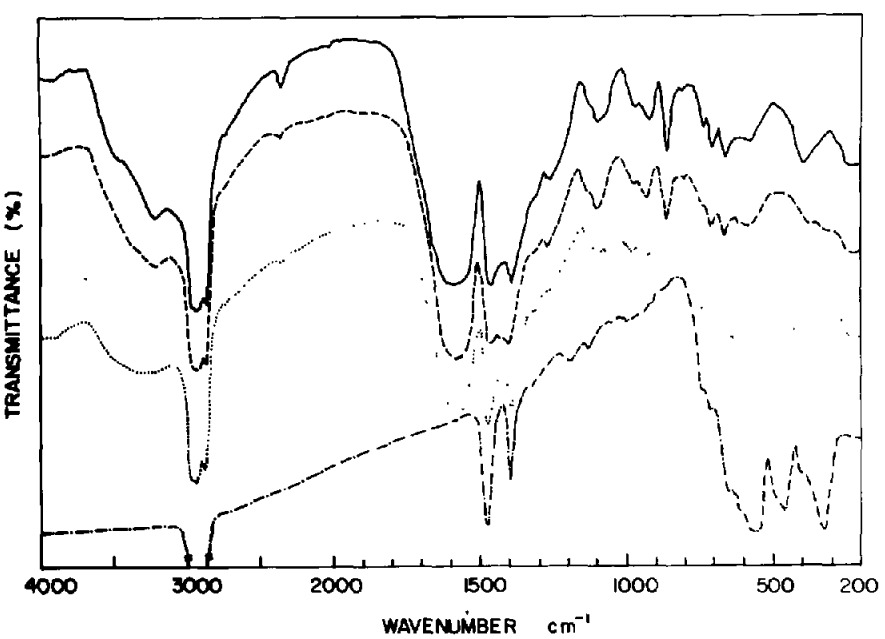

Fig. 2. IR spectra of the decomposition steps of iron citrate, (——) step A, (- - - - -) step B, (· · · · · ·) step C, (· — · — ·) step D.

The IR spectrum (Fig. 2) of the product obtained at the end of the fourth step of the decomposition curve (step D) showed a complete absence of all the bands due to citrate and the appearance of new and strong bands in the oxide region of the IR spectrum. These oxide bands which prominently occur at 560, 460, 400 and 320 cm^{-1} are found to compare with those of the α-phase of iron oxide [4]. The formation of this α-Fe_2O_3 as the final product of decomposition was also confirmed by XRD (Table 2). The observed weight loss of 17.0% in this exothermic step with an activation energy of 31.5 kcal mol^{-1} in the temperature range 330–460°C is therefore due to the total loss of all the organic material and it agrees with the calculated weight loss of 18.1% required for the formation of iron oxide.

As is clear from the above discussion the IR spectra of the various decomposition steps do not show the appearance of any new bands up to the third step. They show only a gradual decrease in the intensity of all the bands present in the IR spectrum of the original sample. This shows that the

TABLE 1

Thermal analysis data for the decomposition of iron citrate

Decomposition step	% Weight loss observed at the end of each step	% Weight loss calculated	Temperature range (°C)	Activation energy (kcal mol^{-1})	Type of each reaction
A	13.0	12.9	22–175	31.8	endothermic
B	20.2	20.0	175–228	10.6	exothermic
C	20.4	20.6	228–330	33.4	exothermic
D	17.0	18.1	330–460	31.5	exothermic

TABLE 2

X-ray diffraction pattern of α-Fe_2O_3 formed as a result of the iron citrate decomposition at 460°C

d reported (Å) α-Fe_2O_3	d observed (Å)	I/I_0
3.68	3.66	mw
2.69	2.68	vs
2.51	2.50	s
2.20	2.20	mw
1.84	1.84	ms
1.69	1.69	ms
1.60	1.60	mw
1.49	1.48	ms
1.45	1.45	mw

vs = very strong, s = strong, ms = medium strong, mw = medium weak, w = weak, vw = very weak.

thermal decomposition of iron citrate results in the gradual burning of the amorphous citrate salt to the crystalline α-phase of iron oxide. The probable intermediates formed during the multistage decomposition of iron citrate are, therefore, as given in the decomposition scheme.

In our earlier work [5] we have already reported the thermal decomposition of barium citrate resulting in stable barium carbonate as the final product. This $BaCO_3$ formation starts at about 300°C and is completed by 412°C. In order to convert this $BaCO_3$ further to barium oxide a very high temperature [6] is required for the removal of one molecule of CO_2 from $BaCO_3$.

As seen from the above discussion, iron citrate, in contrast to barium citrate, decomposes directly to iron oxide without the formation of a stable carbonate intermediate. This is confirmed by the absence of bands due to carbonate in the IR spectra of the various decomposition steps.

The simultaneous decomposition of iron citrate and barium citrate showed further interesting results. When a mixture of the citrates of iron and barium in the required stoichiometric proportion is heated, gradual decomposition of the mixture similar to that of iron citrate takes place at every stage of decomposition. The IR spectra of the product at the end of every decomposition step show a subsequent reduction in the intensities of the citrate bands. There is no appearance of any new bands in the spectra up to a temperature of about 300°C. X-ray diffraction patterns of the decomposition product at 400 and 500°C showed lines (Table 3) which corresponded to either γ-Fe_2O_3 or Fe_3O_4 or a mixture of these two. As the d values of γ-Fe_2O_3 and Fe_3O_4 are very close it is very difficult to distinguish between the two oxides. The observation is, however, contrary to that observed in the individual decomposition of iron citrate wherein α-Fe_2O_3 is formed as the end product. No X-ray diffraction lines due either to barium carbonate or oxide were ob-

TABLE 3

X-ray diffraction pattern resulting from the decomposition of the iron citrate and barium citrate mixture at 500°C

d reported (Å) Fe_3O_4	I/I_0 Fe_3O_4	d reported (Å) γ-Fe_2O_3	I/I_0 γ-Fe_2O_3	d observed (Å)	I/I_0 observed
2.97	mw	2.95	mw	2.93	ms
–	–	2.78	w	–	–
2.53	vs	2.52	vs	2.51	vs
2.42	w	2.41	vw	–	–
2.10	mw	2.08	mw	2.08	mw
1.71	mw	1.70	w	1.69	w
1.61	ms	1.61	ms	1.60	mw
1.48	s	1.48	ms	1.47	ms

vs = very strong, s = strong, ms = medium strong, mw = medium weak, w = weak, vw = very weak.

served as the amount of barium was beyond the X-ray detection limit. Also, since the IR spectra of the same products did not show any bands due to carbonate, the possibility of the formation of iron carbonate or barium carbonate can easily be ruled out. This leads to the conclusion that barium citrate, instead of decomposing to $BaCO_3$, has decomposed directly to BaO in the presence of iron oxide. This observation is again in contrast to the individual decomposition of barium citrate wherein BaO is formed via the $BaCO_3$ intermediate at very high temperatures. Therefore, at 400°C complete decomposition of the organic material takes place forming iron oxide (other than α-Fe_2O_3) and BaO which subsequently combine with each other resulting in the formation of barium ferrite at 600°C. This barium ferrite formation was confirmed by XRD (Table 4). The X-ray diffraction pattern recorded at 650°C also shows the formation of barium ferrite. Of course, the ferrite formed at 650°C was more crystalline than that obtained at 600°C. Thus, at the end of the thermal decomposition of the mixture, the organic portion is removed, leaving the selected composition of mixed oxides chemically combined.

As seen in the foregoing discussion, barium ferrite, prepared by the liquid mix technique, is formed at 600°C. This temperature of formation of barium ferrite is lower than that at which the ferrite is formed when prepared by the conventional ceramic method [7] or even the other methods like the coprecipitation method [8]. This low temperature formation of barium ferrite itself reflects the greater reactivity and purity of the iron and barium oxides formed as a result of the citrate decompositions.

Decomposition scheme of iron citrate

$$(1)\ FeC_6H_5O_7 \cdot 2H_2O \xrightarrow[-2H_2O]{22-175^\circ C} FeC_6H_5O_7$$

TABLE 4

X-ray diffraction pattern of barium ferrite formed at 600°C

d reported (Å)	d observed (Å)	I/I_0	d reported (Å)	d observed (Å)	I/I_0
3.86	3.83	w	1.94	1.94	vw
2.93	2.92	ms	1.81	1.81	w
2.77	2.76	s	1.71	1.71	w
2.61	2.61	s	1.66	1.66	ms
2.53	2.53	mw	1.62	1.62	ms
2.41	2.41	ms	1.46	1.47	ms
2.22	2.22	ms	1.42	1.42	vw
2.12	2.12	mw	1.39	1.39	w
			1.31	1.30	w

s = strong, ms = medium strong, mw = medium weak, w = weak, vw = very weak.

$$(2)\ FeC_6H_5O_7 \xrightarrow[-C\ (as\ CO,\ CO_2)]{175-228^\circ C,\ -CO_2} Fe(OH)\cdot(CH_2COO)_2$$

$$(3)\ Fe(OH)\cdot(CH_2COO)_2 \xrightarrow[-C\ (as\ CO,\ CO_2)]{228-330^\circ C,\ -CO_2,\ -2H} FeO(CH_3COO)$$

$$(4)\ FeO(CH_3COO) \xrightarrow[-2C\ (as\ CO,\ CO_2)]{330-460^\circ C,\ -1.5O,\ -3H} 1/2Fe_2O_3$$

ACKNOWLEDGEMENTS

We are grateful to Dr. C.I. Jose for his helpful discussions regarding the IR work. One of the authors (A.S.) thanks the Indian National Science Academy for the award of a fellowship during the course of this work and the Director, National Chemical Laboratory, for providing laboratory facilities.

REFERENCES

1 N.G. Eror, Jr. and T.M. Loehr, J. Solid State Chem., 12 (1975) 319.
2 E.F. Funkenbusch, P. Singh and B.C. Cornilsen, Proc. Powder Processing Symp., Joint AIME–Am. Ceram. Soc. Meet., 1981, Louisville, KY, American Institute of Mining and Metallurgical Engineers, to be published.
3 E.S. Freeman and B. Carrol, J. Phys. Chem., 62 (1958) 394.
4 R.A. Nyquist and R.O. Kagel, Infrared Spectra of Inorganic Molecules, Academic Press, London, 1971, p. 79.
5 A. Srivastava, P. Singh, V.G. Gunjikar and C.I. Jose, Thermochim. Acta, 76 (1984) 249.
6 C.D. Hodgman, Handbook of Chemistry and Physics, Chemical Rubber Publishing Co., Cleveland, OH, 1958, p. 538.
7 M. Erchak, Jr., I. Fankuchen and R. Ward, J. Am. Chem. Soc., 68 (1946) 2085.
8 K. Haneda, C. Miyakawa and H. Kojima, J. Am. Ceram. Soc., 57 (1974) 354.